First-principles study of magnetic ordering of an Al infinite single-row atomic wire

2009 J. Phys.: Condens. Matter 21 064240

(http://iopscience.iop.org/0953-8984/21/6/064240)

J. Phys.: Condens. Matter **21** (2009) 064240 (5pp) doi:10.1088/0953-8984/21/6/064240

First-principles study of magnetic ordering of an Al infinite single-row atomic wire

Tadashi Ota[1], **Kikuji Hirose**[1] **and Tomoya Ono**[1,2]

[1] Department of Precision Science and Technology, Osaka University, Suita, Osaka 565-0871, Japan
[2] Research Center for Ultra-Precision Science and Technology, Osaka University, Suita, Osaka 565-0871, Japan

E-mail: ota@cp.prec.eng.osaka-u.ac.jp

Received 20 July 2008, in final form 1 December 2008
Published 20 January 2009
Online at stacks.iop.org/JPhysCM/21/064240

Abstract
In this paper we present a detailed analysis of the atomic and spin-electronic structure of an Al infinite single-row atomic wire (Al-ISAW). Our work is based on *ab initio* self-consistent field calculations within the local density approximation, and we predict structural transformations during elongation using the norm-conserving (NC) and projector augmented-wave (PAW) pseudopotentials. The results obtained by the NC pseudopotential are in good agreement with those obtained by the PAW pseudopotential. We confirm that the Al-ISAW shows a metal–insulator transition and fractures when elongated beyond the equilibrium length. Then, a wire with antiferromagnetic ordering is found to be the lowest energetically. We find that the magnitude of spin polarization in the vicinity of nuclei is marginal and does not play an important role in the Peierls instability. The present results show that the NC pseudopotential can give an accurate physical picture of the atomic and spin-electronic structures of the Al-ISAW.

1. Introduction

One-dimensional (1D) systems of single-row monatomic wires are the ultimate simple model, making them an ideal test ground for developing our understanding of nanoscale phenomena and properties unknown in higher dimensions [1]. It is fundamentally important to know the atomic and spin-electronic structures of monatomic wires. The stability of suspended gold wires and their atomic structures have been investigated theoretically [2–10]. First-principles calculations by Sánchez-Portal *et al* indicated that infinite dimerized wires with a zigzag geometry are energetically favorable, and a Peierls dimerization instability is observed [2]. In several studies it was reported that the conductance of gold wires shows a peak at approximately 1 G_0 (where $G_0 = 2e^2/h$, e being the charge of an electron and h the Planck constant), and an oscillatory evolution of conductance with a period of one atom is observed [9]. In the case of gold wires, the basic mechanism of the Peierls transition can be understood because they have only s-type valence orbitals. However, the situation may be more complex in the case of monatomic wires made of multivalent atoms [6, 11–22]. For example, several studies have shown that an Al wire exhibits more complicated and interesting features: Ayuela *et al* revealed that straight Al wires become magnetic upon elongation and spontaneously deform to zigzag wires with lower magnetization when relaxing [18]. They also demonstrated that dimerization does not occur. The calculation by Sen *et al* showed that a zigzag Al infinite single-row atomic wire (Al-ISAW) is the most stable of the planar structures in the case of a small interatomic distance [19]. Thygesen *et al* recently reported that the conductance of Al wires suspended between electrodes oscillates with a period of four atoms as the wire length is varied [20]. We also investigated the conduction properties of a wire of three Al atoms sandwiched between electrodes during elongation [21]. We found that the electronic conductance of the Al wire is $\sim 1 G_0$ and that it traces a convex downward curve before the wire breaks.

In a previous study [22], we investigated the relation between the atomic and spin-electronic structures of a straight Al-ISAW by first-principles calculations using a

conventional norm-conserving (NC) pseudopotential [23], and we revealed that the Al-ISAW exhibits nanoscale magnetic ordering. However, the NC pseudopotential ignores the behavior of electrons in the vicinity of nuclei and cannot evaluate the exchange–correlation energy with sufficiently high accuracy. For example, care must be taken to construct pseudo augmentation functions for systems with large magnetic moment. In this paper, we investigate the electronic structure and magnetic orderings of an Al-ISAW using the NC [23] and projector augmented-wave (PAW) [24] pseudopotentials. The PAW pseudopotentials enable us to accurately obtain the magnetic orderings of systems without increasing the computational effort. We examine the difference and correspondence between the results obtained by the NC and PAW pseudopotentials. We find that the elongated Al-ISAW exhibits a phase transition with increasing interatomic distance. The difference in the wire lengths of the phase transition obtained by the NC and PAW pseudopotentials is approximately 1 per cent. We also find that the total energy of a trimerized wire with antiferromagnetic (AFM) ordering is the lowest energetically and the NC pseudopotentials give results that are in general as accurate as those obtained with the PAW pseudopotentials in the case of an Al-ISAW. The main reason for this agreement is that the contribution of spin polarization near the nuclei is small; thus, the NC pseudopotentials are capable of handling these cases with good accuracy.

The rest of this paper is organized as follows: the computational method of our study is outlined in section 2, and the results for the Al-ISAW are presented in section 3. Finally, in section 4, we summarize our results.

2. Method

Our calculations were performed within the framework of the local spin-density approximation in density functional theory [25]. We use the real-space finite-difference method [26–29], which allows us to calculate the electronic ground state and the optimized geometry of systems with a high degree of accuracy. The electron–ion interactions are replaced by the NC pseudopotentials of Troullier and Martins [23] or by the PAW pseudopotentials [24]. The wavefunction cutoff is chosen as 27 Ryd, which corresponds to a grid spacing of 0.32 Å, with a higher cutoff energy of 247 Ryd in the vicinity of nuclei with the augmentation of double-grid points [27–29]. The system is modeled within the supercell approach by periodically repeated wires. The size of the supercell is taken as $L_x = L_y = 12.70$ Å and $L_z = N_{\mathrm{atom}} \times d$ where the x and y directions are perpendicular to the wire axis, the z axis is along the wire axis, N_{atom} is the number of Al atoms, and d is the average interatomic distance between adjacent atoms. We carry out sampling using 120 k_z points in the irreducible Brillouin zone of the regular wire, where convergence of the k_z points is assured.

3. Results and discussion

First we examine the differences in some physical quantities of the Al-ISAW in the results obtained by the NC and PAW pseudopotentials. The total energy, the restoring force, and the magnetic moment as functions of interatomic distance are shown in figures 1(A)–(C), respectively. The ground-state electronic structure of the Al-ISAW is ferromagnetic (FM) ordering in both cases. The minimum total energy at

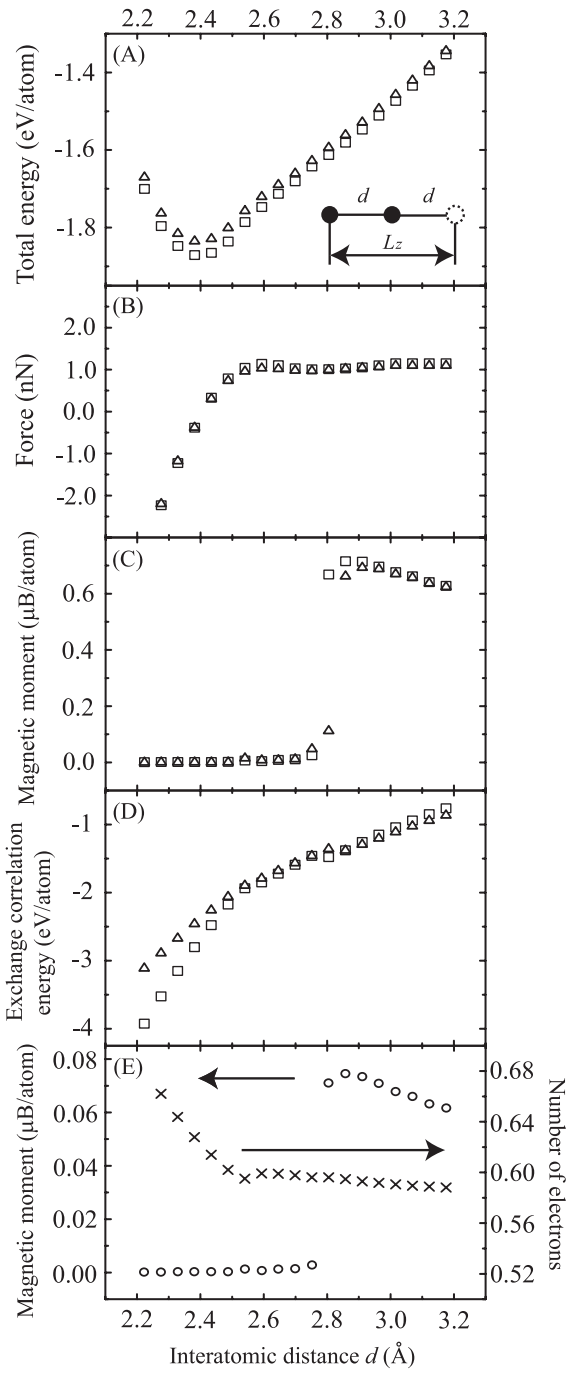

Figure 1. (A) Total energy, (B) restoring force, (C) magnetic moment per atom, (D) exchange–correlation energy, and (E) magnetic moment and the number of electrons in the augmented sphere of the PAW pseudopotential. The $N_{\mathrm{atom}} = 2$ supercell is employed. Zero energy is chosen to be the total energy of an isolated Al atom. In (A)–(D), the squares and triangles indicate the results of the PAW and NC pseudopotentials, respectively. In (E), the circles (crosses) represent the magnetic moment (the number of electrons). The inset in (A) schematically shows the computational model.

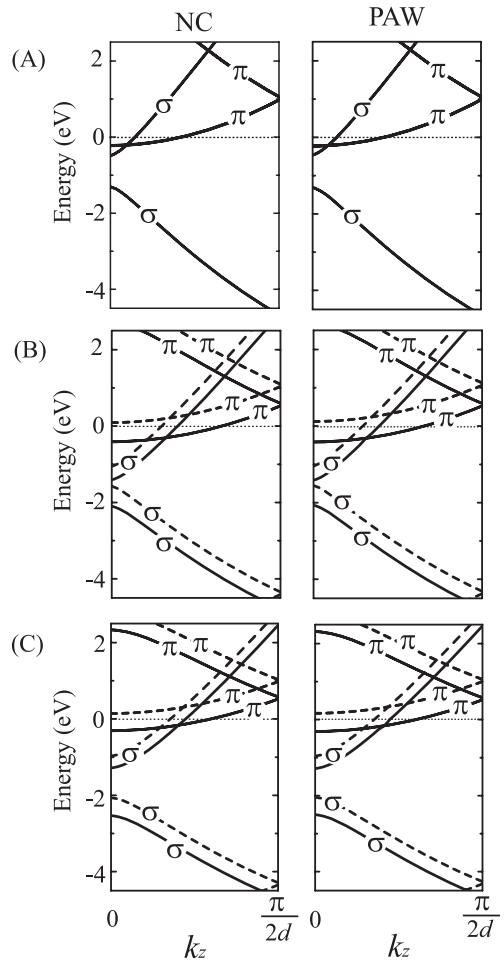

Figure 2. Energy band structures of Al-ISAW along the wire direction at (A) $d = 2.65$ Å, (B) $d = 2.96$ Å, and (C) $d = 3.12$ Å. The $N_{\text{atom}} = 2$ supercell is employed. The result of the NC (PAW) pseudopotential is denoted in the left (right) panel. The solid and dashed curves represent up-spin and down-spin electron bands, respectively. Zero energy is taken to be the Fermi level.

$d = 2.38$ Å obtained by the NC pseudopotential is in fair agreement with that obtained by the PAW pseudopotential. The agreement between both the pseudopotentials is also excellent for the restoring force, as shown in figure 1(B). During the elongation, the magnetic moment is negligible at interatomic distances smaller than 2.80 Å. The magnetic moment then suddenly grows with increasing interatomic distance and saturates at a value of 0.7 μ_{B}/atom. In order to investigate the critical wire length for the phase transition, the change in the spin-electronic structures is examined by increasing the interatomic distances between $d = 2.75$ and 2.86 Å. Then, the critical wire lengths obtained by the NC and PAW pseudopotentials are found to be $d = 2.81$ Å and $d = 2.78$ Å, respectively. To explore the spin-electronic structure in more detail, the energy band structures are depicted in figure 2. The band structures obtained by the NC and PAW pseudopotentials are consistent. The crossing points between the Fermi level and the energy bands are closely related to the atomic configuration of the fractured wire [22]. One can see that the crossing points obtained by the NC pseudopotential coincide with those obtained by the PAW pseudopotential.

Next, to confirm the atomic configuration after the fracture reported in [22], we calculate the atomic and spin-electronic structures of the fractured wires using a large supercell of $N_{\text{atom}} > 2$. Here, we assume three geometrical transitions—dimerization, trimerization, and tetramerization as shown in figure 3—and three magnetic orderings—paramagnetic (PM), FM, and AFM. The interatomic distance of the equally spaced wire is chosen to be 2.96 Å, corresponding to that in [22]. In the case of the trimerized ISAW, the middle atoms are located at the center of the edge atoms. For the tetramerized ISAW, the two middle atoms are allowed to relax, while the two edge atoms are frozen so as to keep the tetramerized configuration. The conclusions obtained from the NC pseudopotential are consistent with those obtained by the PAW pseudopotential: the total energy of the trimerized wire with AFM ordering is the lowest energetically. The total energy of the dimerized wire increases with decreasing atomic distance of the dimers in all the magnetic orderings, which means that no dimerization occurs after the fracture of the wire. In contrast to the results obtained using the generalized gradient approximation in [22], small humps are observed in the trace of the total energy of the tetramerized wire with FM ordering. This is due to the difference of the exchange–correlation function employed in the calculations.

As mentioned before, the atomic configuration of the fractured wire is relevant to the crossing points between the Fermi level and energy bands [22]. The elongated Al-ISAW have doubly degenerate π-symmetry bands and nondegenerate σ-symmetry bands as shown in figure 2(B). The π- and σ-symmetry bands cross the Fermi level at $k_z \approx \frac{\pi}{3d}$ and $k_z \approx \frac{\pi}{6d}$, respectively. Thus, one can predict that the fractured atomic configuration with magnetic ordering has a 6d periodicity. The trimerized wire with AFM ordering has a 6d periodicity, while that with FM ordering has a 3d periodicity. The electronic band structures for the trimerized wires with AFM and FM orderings are plotted in figure 4. In the case of AFM ordering, the energy band structure exhibits an energy gap at $k_z = \frac{\pi}{6d}$ and Peierls instability. On the other hand, in the case of FM ordering, the σ-symmetry bands cross the Fermi level at $k_z \approx \frac{\pi}{6d}$ and the wire still shows metallic behavior. The electronic structures computed using the NC pseudopotential are in good agreement with those obtained using the PAW pseudopotential.

The major difference in the computational effort required for the NC and PAW pseudopotentials is the treatment of the exchange–correlation energy. In particular, the magnetic moment and the number of electrons near the nuclei are important for the difference. However, the above results imply that the contribution of the wavefunction near the nuclei does not play a crucial role in the Peierls instability of the Al-ISAW. To verify this fact, the exchange–correlation energy of the wires is shown in figure 1(D). For the wire with a length of more than $d = 2.54$ Å, both pseudopotentials give similar results for the exchange–correlation energy. However, unlike the exchange–correlation energy, the total energy does not exhibit a large variation due to the phase transition. This is because the phase transition significantly influences not only the spin configuration but also the occupation number of the π- and σ-symmetry bands. The phase transition

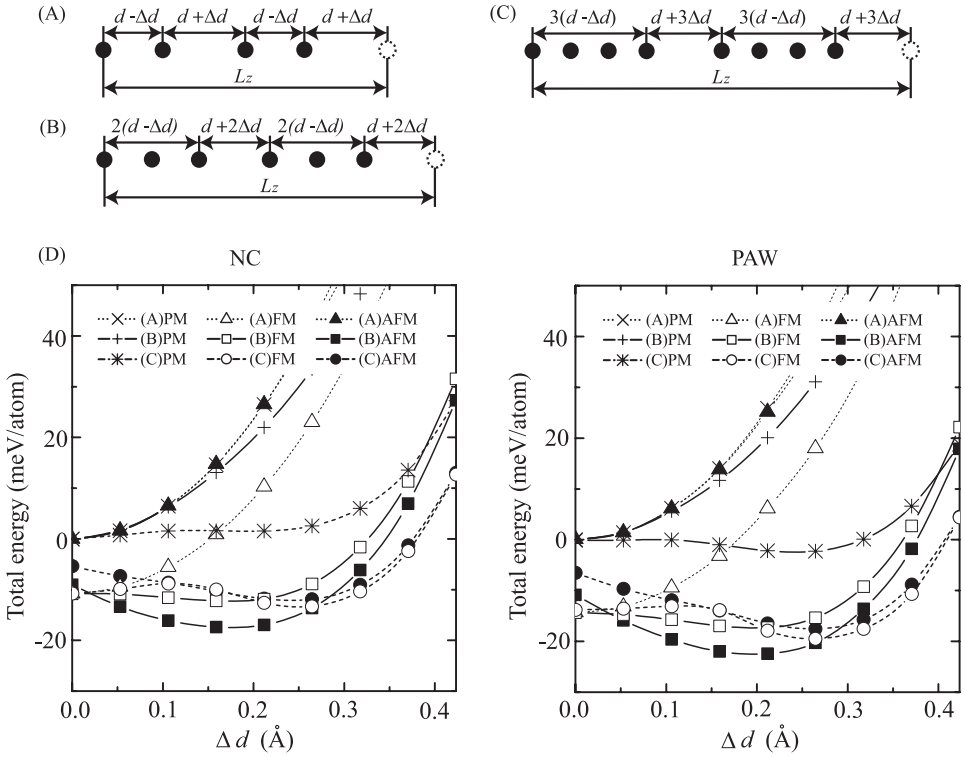

Figure 3. Models for (A) dimerized wire with $N_{\rm atom} = 4$, (B) trimerized wire with $N_{\rm atom} = 6$, and (C) tetramerized wire with $N_{\rm atom} = 8$. (D) Total energy per atom as a function of the bond length in the wire with PM, FM, and AFM orderings. Zero energy is taken to be the total energy of the wire with PM ordering at $\Delta d = 0$ Å. The average interatomic distance d is set to be 2.96 Å. In (A)–(C), the closed circles denote the atoms in a supercell and the open ones show the replicated atoms in the adjacent supercell. In (D), the left (right) panel is calculated by the NC (PAW) pseudopotential.

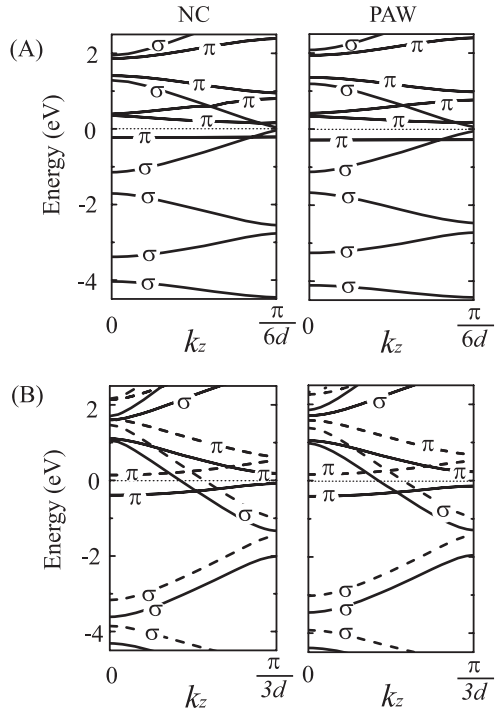

Figure 4. Energy band structures of a fractured Al-ISAW at $\Delta d = 0.21$ Å with $d = 2.96$ Å. (A) trimerized wire with AFM ordering. (B) trimerized wire with FM ordering. The left (right) panel is calculated with the NC (PAW) pseudopotential. The solid and dashed curves represent up-spin and down-spin electron bands, respectively. Zero energy is taken to be the Fermi level.

also produces large changes in the Hartree energy and the exchange–correlation energy. Because the variations of the Hartree energy and the exchange–correlation energy cancel out in this system, a significant change in the total energy is not found. On the other hand, in the case of wires with the length of no more than $d = 2.54$ Å, a slight difference between the two pseudopotentials occurs for the exchange–correlation energy. In figure 1(E), we plot the magnetic moment and the number of electrons within the augmentation sphere of the PAW pseudopotential $\Omega_{\rm R}$, where the radius of $\Omega_{\rm R}$ is chosen to be 0.95 Å. Contrary to the NC pseudopotentials, the PAW pseudopotential is an all-electron potential, giving access to the true wavefunctions and the full electron density. Therefore, the PAW pseudopotentials can provide accurate spin-electronic structures around nuclei. The magnetic moment and the number of electrons are defined as $\int_{\Omega_{\rm R}} (\rho_\uparrow(r) - \rho_\downarrow(r))\,{\rm d}r$ and $\int_{\Omega_{\rm R}} (\rho_\uparrow(r) + \rho_\downarrow(r))\,{\rm d}r$, respectively. As shown in figure 1(E), the slight difference in the exchange–correlation energy is due to the increase in the number of electrons for wires with the length of no more than $d = 2.54$ Å. Furthermore, in figure 1(E), the magnetic moment within $\Omega_{\rm R}$ is one-tenth of the total magnetic moment per atom, while the number of electrons within $\Omega_{\rm R}$ is one-fifth of the total number of electrons. The magnitude of the spin polarization in the augmented sphere is small. Thus, the determination of magnetic ordering is feasible in calculations using NC pseudopotentials.

4. Summary

First-principles calculations have been performed using NC and PAW pseudopotentials to study the atomic and spin-electronic structures of an Al-ISAW. We have elucidated that the conclusions derived from the calculations using the pseudopotentials are consistent. We have also found that the magnitude of spin polarization in the augmented sphere of the PAW pseudopotential is small in the case of an elongated Al-ISAW, and its influence on the Peierls instability is not crucial. As a result, the NC pseudopotential is able to reproduce the total energy, restoring force, magnetic moment, and the fractured atomic configuration, which agree with those obtained using the PAW pseudopotential.

Acknowledgments

The authors thank Professor S Blügel and Dr N Atodiresei of the Forschungszentrum Jülich, Germany for providing the database of the PAW pseudopotentials. This research was partially supported by a Grant-in-Aid for the 21st Century COE 'Center for Atomistic Fabrication Technology', by a Grant-in-Aid for Scientific Research in Priority Areas 'Development of New Quantum Simulators and Quantum Design'(grant no. 17064012), and also by a Grant-in-Aid for Young Scientists (B) (grant no. 20710078) from the Ministry of Education, Culture, Sports, Science and Technology. The numerical calculations were carried out using the computer facilities at the Institute for Solid State Physics at the University of Tokyo, the Research Center for Computational Science at the National Institute of Natural Science, and the Information Synergy Center at Tohoku University.

References

[1] Kouwenhoven L P, Schön G and Sohn L L 1997 *Mesoscopic Electron Transport* vol 345 (Dordrecht: Kluwer) pp 1–44 and references therein
[2] Sánchez-Portal D, Artacho E, Junquera J, Ordejón P, García A and Soler J M 1999 *Phys. Rev. Lett.* **83** 3884
[3] Okamoto M and Takayanagi K 1999 *Phys. Rev.* B **60** 7808
[4] Häkkinen H, Barnett R N, Scherbakov A G and Landman U 2000 *J. Phys. Chem.* B **104** 9063
[5] Tsukamoto S, Ono T, Fujimoto Y, Inagaki K, Goto H and Hirose K 2001 *Mater. Trans. JIM* **42** 2257
[6] Palacios J J, Pérez-Jiménez A J, Louis E, SanFabián E and Vergés J A 2002 *Phys. Rev.* B **66** 035322
[7] Fujimoto Y and Hirose K 2003 *Phys. Rev.* B **67** 195315
[8] da Silva E Z, Novaes F D, da Silva A J R and Fazzio A 2004 *Phys. Rev.* B **69** 115411
[9] Lee Y J, Brandbyge M, Puska M J, Taylor J, Stokbro K and Nieminen R M 2004 *Phys. Rev.* B **69** 125409
[10] Ono T and Hirose K 2005 *Phys. Rev. Lett.* **94** 206806
[11] Kobayashi N, Brandbyge M and Tsukada M 2000 *Phys. Rev.* B **62** 8430
[12] Kobayashi N, Aono M and Tsukada M 2001 *Phys. Rev.* B **64** 121402
[13] Jerlínek P, Pérez R, Ortega J and Flores F 2003 *Phys. Rev.* B **68** 085403
[14] Okano S, Shiraishi K and Oshiyama A 2004 *Phys. Rev.* B **69** 045401
[15] Asari Y, Nara J, Kobayashi N and Ohno T 2005 *Phys. Rev.* B **72** 035459
[16] Fujimoto Y, Asari Y, Kondo H, Nara J and Ohno T 2005 *Phys. Rev.* B **72** 113407
[17] Xu Y, Shi X, Zeng Z, Zeng Z Y and Li B 2007 *J. Phys.: Condens. Matter* **19** 056010
[18] Ayuela A, Raebiger H, Puska M J and Nieminen R M 2002 *Phys. Rev.* B **66** 035417
[19] Sen P, Ciraci S, Buldum A and Batra I P 2001 *Phys. Rev.* B **64** 195420
[20] Thygesen K S and Jacobsen K W 2003 *Phys. Rev. Lett.* **91** 146801
[21] Ono T and Hirose K 2004 *Phys. Rev.* B **70** 033403
[22] Ono T and Hirose K 2003 *Phys. Rev.* B **68** 045409
[23] Troullier N and Martins J L 1991 *Phys. Rev.* B **43** 1993
[24] Blöchl P E 1994 *Phys. Rev.* B **50** 17953
[25] Vosko S H, Wilk L and Nusair M 1980 *Can. J. Phys.* **58** 1200
[26] Chelikowsky J R, Troullier N and Saad Y 1994 *Phys. Rev. Lett.* **72** 1240
[27] Ono T and Hirose K 1999 *Phys. Rev. Lett.* **82** 5016
[28] Ono T and Hirose K 2005 *Phys. Rev.* B **72** 085115
[29] Hirose K, Ono T, Fujimoto Y and Tsukamoto S 2005 *First-Principles Calculations in Real-Space Formalism, Electronic Configurations and Transport Properties of Nanostructures* (London: Imperial College Press)